Optical Ultrasound Imaging for Endovascular Repair of Abdominal Aortic Aneurysms: A Pilot Study

Callum Little[1][0000-0002-2267-0924], Shaoyan Zhang[1][0000-0002-9563-2873],
Richard Colchester[1][0000-0001-8657-0546], Sacha Noimark[1][0000-0002-5351-4633],
Sunish Mathews[1][0000-0002-2289-3669], Edward Zhang[1][0000-0003-3717-1367],
Paul Beard[1][0000-0001-7710-2759], Malcolm Finlay[2][0000-0001-6403-9340],
Tara Mastracci[2][0000-0002-2532-8614], Roby Rakhit[3][0000-0002-0108-8169],
Adrien Desjardins[1][0000-0002-1932-1811]

[1] University College London, London, UK
[2] Barts Heart Centre, London, UK
[3] Royal Free Hospital, London, UK
a.desjardins@ucl.ac.uk

Abstract. An abdominal aortic aneurysm (AAA) is a persistent localized dilatation of the aorta to more than 1.5 times the expected diameter, which may lead to rupture with resultant high mortality. Endovascular repair (EVAR) of AAAs is a minimally invasive procedure that involves the peripheral delivery of one or more covered endografts to the aneurysmal segment, via a catheter-based system. A particularly challenging group of patients to treat are those in which the aneurysmal sac extends proximally to include the origin of the renal arteries (15% of all AAAs). To maintain the patency of renal side branches in these "complex" cases, *in situ* fenestration (ISF) of endografts during AAA procedures has been proposed. The challenges addressed in this study were a) to develop an endovascular imaging system for visualizing side branches beyond deployed endografts and thereby to determine the locations for ISF; b) to obtain an initial assessment of the clinical utility of this system. Here, all-optical ultrasound (OpUS) imaging with a fiber optic transducer was used for real-time guidance, wherein ultrasonic pulses are generated in nanocomposite coatings via the photoacoustic effect and received optically using a Fabry-Perot cavity. These custom OpUS transducer components were integrated into a steerable sheath (6 Fr) that also included a separate optical fiber for delivering laser pulses for fenestrating the endograft. In an ex-vivo model, it was shown that OpUS imaging extended through the endograft and underlying aortic tissue, and permitted aortic side-branch visualization. During an EVAR procedure in a porcine model *in vivo*, an aortic side branch was visualized with OpUS imaging after the endograft was deployed and optical fenestration of the stent graft was successfully performed. This study showed that OpUS is a promising modality for guiding EVAR and could find particularly utility with identifying aortic side branches for ISF during treatment of complex AAAs.

Keywords: Optical ultrasound imaging, abdominal aortic aneurysm, endovascular repair.

1   Introduction

Intervention options for the treatment of abdominal aortic aneurysms (AAAs) include open surgery or endovascular repair (EVAR). A minimally invasive procedure, EVAR involves the peripheral delivery of one or more covered endografts to the aneurysmal segment via a catheter-based system. EVAR has been demonstrated to be superior to open surgery with regards to early mortality [1, 2]. A particularly challenging group of patients to treat are those in which the aneurysmal sac extends proximally to include the origin of the renal arteries. These are known as juxtarenal or "complex" AAAs and account for roughly 15% of all AAAs [3].

With complex AAA repair, it is of paramount importance to maintain the patency of major aortic side branches to allow for end-organ perfusion. Traditionally, open surgery was preferred for these complex cases; however, with the advent of endografts that have pre-made openings (fenestrations) in the graft material, these patients can be treated using fenestrated endovascular repair (FEVAR). The concept of *in situ* fenestration (ISF) for endografts during FEVAR has been proposed as an alternative to the use of pre-fenestrated endografts. With ISF, the fenestrations are generated within the aorta following deployment of the endograft. Potential benefits of this approach include both greater anatomical conformity and reduced device cost. Once ISF has been performed, a wire is passed through the fenestration into the side-branch. The fenestration is then dilated with incrementally sized non-compliant or cutting balloons and secured with a stent that maintains communication between the aorta and side-branch [4]. Several fenestration methods have been proposed, of which mechanical puncture and thermal ablation of stent material are the most prominent. Thermal ablation methods for ISF are attractive as there is no requirement to exert penetrative force on the endograft material. Instead, the material is vaporized through the use of radiofrequency (RF) [5] or laser energy, in which 94% success was achieved in 16 patients with no major complications [6].

A key challenge with ISF that we address here is to visualize aortic side branches in order to precisely identify the locations for fenestration. Pre-procedural imaging in concert with X-ray fluoroscopy can be used for guidance [7]; however, distortion of the aorta due to deployment of the endograft limits the accuracy of this technique [8]. All-optical ultrasound (OpUS) is an emerging imaging modality that involves the optical generation and reception of ultrasound [9], which can be performed with fiber optics that are readily integrated into medical devices [10]. OpUS is a potentially attractive option for guiding ISF for several reasons: the depth penetration achieved for OpUS (>1 cm) is relevant to aneurysmal vessels, high bandwidths enable high resolution imaging (*ca.* 50-100 μm), and a blood-free environment is not required for image acquisition. The feasibility of visualizing aortic side branches with OpUS has previously been demonstrated [9, 11] and intracardiac imaging *in vivo* has been performed [10]. In this study, we explore the application of OpUS to EVAR and ISF, by addressing two open questions: does this technique permit visualization of side branches through endograft material, and can the optical transducers be integrated into a steerable sheath with forward imaging that also permits optical fenestration?

2 Methods

2.1 Device Design

The custom device comprised two primary fiber optic components which were integrated within a catheter: 1) an OpUS transmitter/receiver pair for visualizing side branches; 2) an ISF fiber for optical fenestration. These optical fibers were secured together using heat shrink and housed within a 6 Fr [inner diameter (ID): 2 mm] catheter (Multipurpose-1, Cordis, Santa Clara, CA, USA), leaving a 0.7 mm diameter channel to allow a 0.014" or 0.018" guidewire to be delivered through a generated fenestration. The catheter was delivered to the endovascular stent graft using a 7 Fr ID steerable sheath (Tourguide, Medtronic, USA), a current standard that allowed for bi-directional 180°/90°deflection with manual control and thereby allowed the catheter to be appropriately positioned to detect side-branches behind the endovascular stent (Fig. 1).
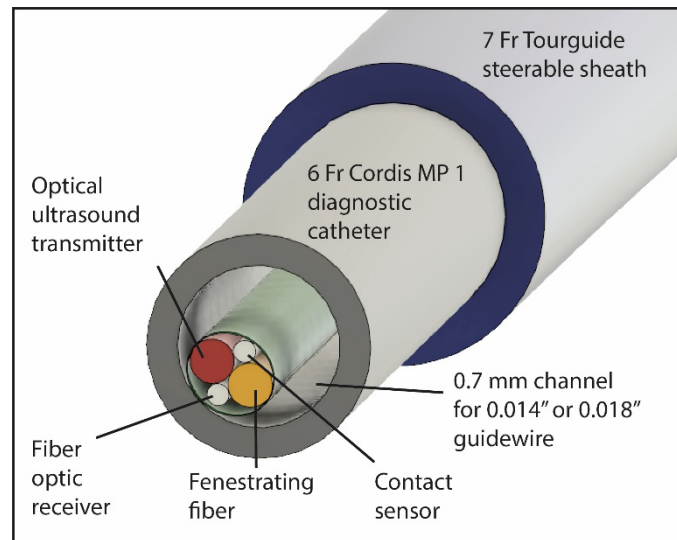

Fig. 1. Custom device for performing all-optical ultrasound imaging and fenestration during endovascular repair (EVAR), shown schematically. The device comprised an optical ultrasound transmitter and receiver for imaging, and a third optical fiber to deliver light for *in situ* fenestration (ISF) of endograft stent material. A custom fiber optic contact sensor was not used in this study. This device was enclosed by heat shrink and positioned within two off-the-shelf, commercially-available devices: a diagnostic catheter and a steerable sheath.

The OpUS transmitter comprised a custom nanocomposite material for photoacoustic generation of ultrasound, with optical absorption of excitation light by a near-infrared absorbing dye embedded within a medical-grade elastomeric host [12] that was applied to a 400 μm circular surface following the design of Colchester et al. [13]. The OpUS receiver comprised a plano-concave microresonator positioned at the distal end

of a fiber. These fiber optic OpUS components were interrogated by a custom console that delivered pulsed excitation multi-mode light to the transmitter (wavelength: 1064 nm; pulse duration: 2 ns; pulse energy: 20.1 μJ; repetition rate: 100 Hz) and wavelength-tunable continuous wave single-mode light to the receiver (1500-1600 nm; 4 mW). This custom console, previously described in detail [9], comprised software for real-time processing and display of concatenated A-scans as M-mode OpUS images. The ISF fiber for fenestration had an inner diameter of 400 μm and transmitted light from a laser unit that permitted control of the pulse duration and power (Diomed D15 Diode, Diomed Holdings, USA; wavelength: 808 nm; maximum power: 4W). This wavelength was chosen to minimize damage to the underlying vascular tissues [14].

2.2   Benchtop Imaging and Fenestration

To assess whether OpUS permits visualization of side branches through endograft material, a benchtop model with ex-vivo swine aorta (Medmeat Ltd, United Kingdom) was used. A section of the aorta was splayed open longitudinally to create a flat surface and secured to a cork board. Endograft stent material (Zenith Flex® AAA, Cook Medical, USA) made from a synthetic polyester Dacron Material (DM) (polyethylene terephthalate) was positioned above the aortic sample. An OpUS imaging scan was performed with 600 lateral steps of length 50 μm using a motorised stage [9].

To test the effects of different laser parameters on optical fenestration, the following were varied: the pulse energy, the pulse duration, and the distance between the distal end of the fenestration optical fiber and the endograft material. Fenestrations with different combinations of these parameters (2.5W, 0.5s; 1.8W, 0.5s; 4.2W, 0.5s; 4.2W, 1s; 4.2W, 5s) were attempted in different sections of aortic tissue. A piece of endograft material was secured above each tissue section; the distance from the endograft material to the tissue was approximately 2 mm. The tissue and endograft material were immersed in anticoagulated sheep blood (TCS Biosciences, Buckingham, UK). A fenestration was deemed to have been successfully achieved if adjacent tissue was visible when the surrounding blood was drained.

2.3   *In Vivo* Imaging and Fenestration

To obtain a preliminary validation of the system's potential for guiding EVAR and ISF, OpUS imaging and endograft fenestration were performed in a clinically realistic environment using an *in vivo* porcine model. The primary objectives of this experiment were a) to visualize an aortic side branch behind a deployed endograft; b) to perform optical fenestration of the endograft. All procedures on animals were conducted in accordance with U.K. Home Office regulations and the Guidance for the Operation of Animals (Scientific Procedures) Act (1986). The protocol for this study was reviewed and ratified by the local animal welfare ethical review board.

Following successful anesthesia, transcutaneous ultrasound (US) was used to gain percutaneous access to both common femoral arteries; 8 Fr vascular sheaths were inserted bilaterally. Both fluoroscopic acquisition and digital subtraction angiography with an iodine-based contrast agent were performed to create a road-map for further

stages of the experiment. The ISF device was inserted via the Right Femoral Artery (RFA) and directed with the steerable catheter into the aorta. The inner catheter of the ISF device was advanced into the aorta.

For the EVAR procedure, a non-fenestrated iliac endograft was used (Zenith Spiral-Z, Cook Medical, USA; proximal/distal diameter: 13 mm/11 mm; length: 129 mm). The choice of an iliac endograft originally for human patients was for the comparatively smaller dimensions of the swine aorta. The sheath in the RFA was up-sized to a 14 Fr in order to accommodate the delivery system. The stent was deployed across the renal artery bifurcation. The ISF device was inserted into the lumen of the endograft and OpUS imaging was performed with a longitudinal pullback across the covered left renal artery. Once positioned over the desired location, a single pulse from the 808 nm fenestration laser (power: 4.2 W; pulse duration: 5 s) was delivered to the endograft to create a fenestration. A coronary guidewire (0.018"; Balanced Middleweight Universal, Abbott, USA) was then inserted through the ISF device and through the fenestration into the side-branch. Expansion of the fenestration in the endograft was then performed with a series of three balloons (2 mm non-compliant, 3 mm non-compliant and 3 mm cutting) to create a fenestration large enough to accommodate a stent. Following successful ISF, the procedure was ended and the ISF device was removed.

3 Results

3.1 Benchtop Imaging and Fenestration

With OpUS imaging of the paired endograft and underlying aortic tissue, the stent graft manifested as an echo-bright linear structure (Fig. 2). Aortic tissue beneath the graft could be imaged to a depth > 6 mm from the transducer surface (> 3 mm from the tissue surface). The pullback revealed the side-branch within the aorta, which was apparent as a well demarcated area with signal drop-out, consistent with an absence of tissue.

During benchtop attempts, a fenestration was successfully created with a pulse duration of 0.5 s and an optical power of 1.8 W when the distal end of the fiber was in contact with the endograft material. This combination of pulse duration and optical power corresponded to the smallest energy that yielded fenestration with this device. There was no macroscopic tissue damage with these parameters. The size of the fenestration increased with both higher power outputs and longer laser pulse durations. When the distal end of the optical fiber was recessed a distance of 3 mm from the endograft material, both a higher power output and longer pulse duration were required to generate a fenestration. No macroscopic tissue damage was identified during any of the fenestration experiments. As a control, the optical fiber was placed directly on the tissue with no stent material. In this configuration, a power of 4.2W and a pulse duration of 5 s resulted in a macroscopic thermal ablation of the tissue.
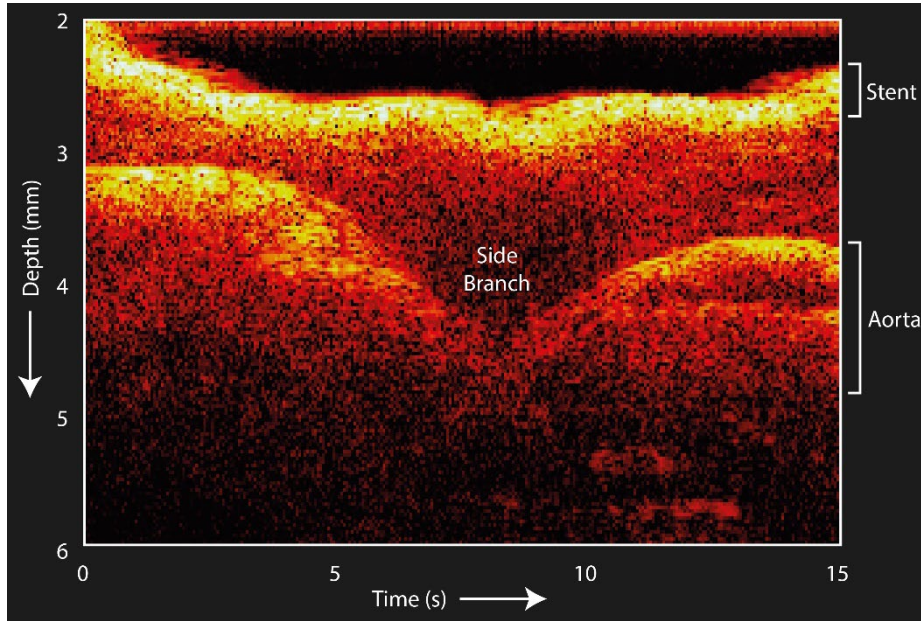
Fig. 2. All optical ultrasound (OpUS) imaging of the endograft paired with underlying aortic tissue, performed on the benchtop. The stent endograft material was strongly hyperechoic. The underlying aorta is apparent as a 2-3 mm thick region. The side-branch presented as an absence of signal, corresponding to a discontinuity in the aortic tissue.

3.2   *In vivo* Imaging and Fenestration

The renal bifurcation was readily observed with fluoroscopic guidance and X-ray con-trast injections. Due to the small diameter of the swine aorta relative to that of an adult human, it proved challenging to achieve sufficient bending of the steerable sheath whilst maintaining a gap between the imaging device and the aortic tissue. In this con-figuration, bend-induced losses in the fiber optic receiver significantly lowered the sig-nal-to-noise (SNR) ratio relative to that obtained during benchtop imaging. Nonethe-less, a manual pullback with imaging performed at a slightly non-perpendicular angle relative to the aortic surface proved feasible. With OpUS imaging during this pullback, the endograft material presented as a strongly hyperechoic region and the underlying aorta could be imaged to a depth > 3 mm. A side branch presented as a hypoechoic region consistent with an absence of tissue within the renal vessel lumen (Fig. 3a).

For ISF, the laser output parameters that were chosen (4.2 W, 5 secs) were intention-ally higher than the minimum values observed in benchtop experiments. Following the ISF, the guidewire was passed into the renal artery. A post-mortem dissection con-firmed a successful optical fenestration (Fig. 3b). Passage of the guidewire through the fenestration in the endograft material was confirmed with fluoroscopic imaging per-formed *in vivo* (Fig. 3c). No tearing in the endograft material that may have arisen from balloon-induced expansion was apparent (Fig. 3b).
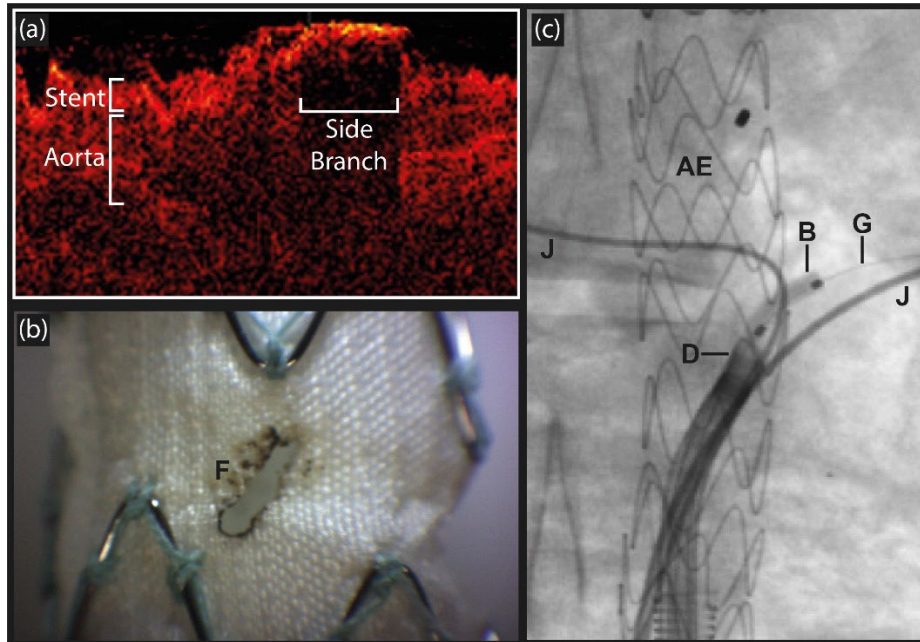
Fig. 3. (a) All-Optical Ultrasound (OpUS) imaging obtained from a manual pullback across a renal bifurcation, formed from concatenated A-scans. The endograft material presents as a hyperechoic region above the underlying aortic tissue; a side branch that manifested as an absence of signal. (b) With optical microscopy of the endograft performed post autopsy, a fenestration (F) is apparent. (c) Fluoroscopic imaging immediately after optical *in situ* fenestration (ISF) showing successful insertion of the guidewire (G) into the renal artery. AE: aortic endograft; D: custom device for optical ultrasound imaging and fenestration; B: balloon inflated to dilated the fenestration; J: J-tip 0.035" wires that mark the location of the renal arteries.

4   Discussion

A key observation of this study is that OpUS offers direct visualization of aortic tissue beneath an AAA endograft, and detection of vascular side-branches. This capability is important for appropriate ISF positioning, thereby maintaining side-branch patency. The ability to detect a side-branch immediately before performing fenestration with the same device could reduce the risk of inappropriate positioning and the subsequent need for conversion to open surgery. In current clinical practice, there is no device that allows for direct imaging of aortic side branches with the added capability of achieving endograft fenestration.

Current methods for generating ISF, although promising, are not guided by intravascular imaging. With these methods, there is a risk of creating a fenestration that is not aligned with the side-branch, leading to a potential endoleak, and a risk of causing injury to underlying tissue structures. The potential cost implication of ISF is significant.

The average costs of pre-fenestrated and patient-specific grafts are ca. £15,400 and £24,000 (GBP), respectively; the cost of a non-fenestrated aortic endograft that could be used for ISF is ca. £6,000.

Several improvements to the device can be envisaged. An increase in the lateral OpUS imaging resolution could be effected with greater US beam collimation, for instance with the use of a larger-diameter transmitting surface; however, this change would likely result in increased device size and reduced flexibility. Improvements in the SNR of OpUS images could potentially be achieved with depth-dependent frequency filtering and with the application of deep-learning methods [15]. In future iterations, imaging and ISF could be performed with a single optical fiber [16, 17], thereby reducing device size, increasing device flexibility/deliverability and potentially reducing device cost. Using the same ultrasonic receiver used for reception during imaging, it could be possible to use ultrasonic tracking to localize the device relative to an external imaging device [15, 18, 19], thereby reducing the dependency on fluoroscopic image guidance and corresponding contrast injections.

During the *in vivo* procedure in this study, the power of the fenestration laser was chosen to be higher than the minimum value observed in the benchtop component of this study to increases the chances of success. It remains to be seen whether a lower output setting may be viable in this context, with the presence of device motion and flowing blood and with pathological changes in the arterial wall. In future studies, real-time feedback from OpUS imaging could be incorporated to determine the power and pulse duration of the fenestrating laser; a similar probe could be used for cardiac ablation, for instance in the context of treatment of atrial fibrillation [20].

This study presented a novel imaging probe for performing interventional image guidance for endovascular procedures. We conclude that OpUS imaging is a promising modality for guiding EVAR; in concert with and optical fenestration, it could find particularly utility with identifying aortic side branches and performing ISF during treatment of complex AAAs.

Acknowledgements

References

1. Prinssen, M., Verhoeven, E.L.G., Buth, J., Cuypers, P.W.M., van Sambeek, M.R.H.M., Balm, R., Buskens, E., Grobbee, D.E., Blankensteijn, J.D.: A randomized trial comparing

conventional and endovascular repair of abdominal aortic aneurysms. New England Journal of Medicine. 351, 1607–1618 (2004).

2. Greenhalgh, R.M.: Comparison of endovascular aneurysm repair with open repair in patients with abdominal aortic aneurysm (EVAR trial 1), 30-day operative mortality results: randomised controlled trial. The Lancet. 364, 843–848 (2004).

3. Jongkind, V., Yeung, K.K., Akkersdijk, G.J.M., Heidsieck, D., Reitsma, J.B., Tangelder, G.J., Wisselink, W.: Juxtarenal aortic aneurysm repair. J Vasc Surg. 52, 760–767 (2010).

4. Eadie, L.A., Soulez, G., King, M.W., Tse, L.W.: Graft durability and fatigue after in situ fenestration of endovascular stent grafts using radiofrequency puncture and balloon dilatation. European Journal of Vascular and Endovascular Surgery. 47, 501–508 (2014).

5. Numan, F., Arbatli, H., Bruszewski, W., Cikirikcioglu, M.: Total endovascular aortic arch reconstruction via fenestration in situ with cerebral circulatory support: an acute experimental study. Interact Cardiovasc Thorac Surg. 7, 535–538 (2008).

6. le Houérou, T., Fabre, D., Alonso, C.G., Brenot, P., Bourkaib, R., Angel, C., Amsallem, M., Haulon, S.: In situ antegrade laser fenestrations during endo-vascular aortic repair. European Journal of Vascular and Endovascular Surgery. 56, 356–362 (2018).

7. Bailey, C.J., Edwards, J.B., Giarelli, M., Zwiebel, B., Grundy, L., Shames, M.: Cloud-based fusion imaging improves operative metrics during fenestrated endovascular aneurysm repair. J Vasc Surg. 77, 366–373 (2023).

8. Koutouzi, G., Sandström, C., Roos, H., Henrikson, O., Leonhardt, H., Falkenberg, M.: Orthogonal rings, fiducial markers, and overlay accuracy when image fusion is used for EVAR guidance. European Journal of Vascular and Endovascular Surgery. 52, 604–611 (2016).

9. Colchester, R.J., Zhang, E.Z., Mosse, C.A., Beard, P.C., Papakonstantinou, I., Desjardins, A.E.: Broadband miniature optical ultrasound probe for high resolution vascular tissue imaging. Biomed Opt Express. 6, 1502–1511 (2015).

10. Finlay, M.C., Mosse, C.A., Colchester, R.J., Noimark, S., Zhang, E.Z., Ourselin, S., Beard, P.C., Schilling, R.J., Parkin, I.P., Papakonstantinou, I., others: Through-needle all-optical ultrasound imaging in vivo: a preclinical swine study. Light Sci Appl. 6, e17103–e17103 (2017).

11. Alles, E.J., Noimark, S., Zhang, E., Beard, P.C., Desjardins, A.E.: Pencil beam all-optical ultrasound imaging. Biomed Opt Express. 7, 3696–3704 (2016).

12. Lewis-Thompson, I., Zhang, S., Noimark, S., Desjardins, A.E., Colchester, R.J.: PDMS composites with photostable NIR dyes for multi-modal ultra-sound imaging. MRS Adv. 7, 499–503 (2022).

13. Colchester, R.J., Alles, E.J., Desjardins, A.E.: A directional fibre optic ultra-sound transmitter based on a reduced graphene oxide and polydimethylsiloxane composite. Appl Phys Lett. 114, 113505 (2019).

14. Piazza, R., Micheletti, F., Condino, S., Magni, G., Berchiolli, R.N., de Simone, P., Ferrari, V., Ferrari, M., Pini, R., Rossi, F.: In situ diode laser fenestration: An ex-vivo evaluation of irradiation effects on human aortic tissue. J Biophotonics. 12, e201900032 (2019).

15. Maneas, E., Hauptmann, A., Alles, E.J., Xia, W., Noimark, S., David, A.L., Arridge, S., Desjardins, A.E.: Enhancement of instrumented ultrasonic tracking images using deep learning. Int J Comput Assist Radiol Surg. 18, 395–399 (2023).

16. Colchester, R.J., Zhang, E.Z., Beard, P.C., Desjardins, A.E.: High-resolution sub-millimetre diameter side-viewing all-optical ultrasound transducer based on a single dual-clad optical fibre. Biomed Opt Express. 13, 4047–4057 (2022).

17. Noimark, S., Colchester, R.J., Poduval, R.K., Maneas, E., Alles, E.J., Zhao, T., Zhang, E.Z., Ashworth, M., Tsolaki, E., Chester, A.H., others: Polydimethylsiloxane composites for

optical ultrasound generation and multimodality imaging. Adv Funct Mater. 28, 1704919 (2018).

18. Mathews, S.J., Shakir, D.I., Mosse, C.A., Xia, W., Zhang, E.Z., Beard, P.C., West, S.J., David, A.L., Ourselin, S., Vercauteren, T., others: Ultrasonic needle tracking with dynamic electronic focusing. Ultrasound Med Biol. 48, 520–529 (2022).

19. Xia, W., West, S.J., Mari, J.-M., Ourselin, S., David, A.L., Desjardins, A.E.: 3D ultrasonic needle tracking with a 1.5 D transducer array for guidance of fetal interventions. In: Medical Image Computing and Computer-Assisted Intervention–MICCAI 2016: 19th International Conference, Athens, Greece, October 17-21, 2016, Proceedings, Part I 19. pp. 353–361 (2016).

20. Zhang, S., Zhang, E.Z., Beard, P.C., Desjardins, A.E., Colchester, R.J.: Dual-modality fibre optic probe for simultaneous ablation and ultrasound imaging. Communications Engineering. 1, 20 (2022).